Higher Rank Interference Effect on Weak Beamforming or OSTBC Terminals

Michal Čierny, Zhi Ding, *Fellow, IEEE,* Risto Wichman

arXiv:1404.1451v2 [cs.IT] 15 Oct 2014

Abstract

User performance on a wireless network depends on whether a neighboring cochannel interferer applies a single (spatial) stream or a multi stream transmission. This work analyzes the impact of interference rank on a beamforming and orthogonal space-time block coded (OSTBC) user transmission. We generalize existing analytical results on signal-to-interference-plus-noise-ratio (SINR) distribution and outage probability under arbitrary number of unequal power interferers. We show that higher rank interference causes lower outage probability, and can support better outage threshold especially in the case of beamforming.

Index Terms

MIMO; beamforming; spatial multiplexing; STBC; OSTBC; interference; outage probability

I. Introduction

Multi-antenna transmission techniques [1] have substantially transformed the modern wireless communications by providing effective diversity means for improving wireless network capacity

This work has been submitted to the IEEE for possible publication. Copyright may be transferred without notice, after which this version may no longer be accessible.

This work was supported by Academy of Finland, National Science Foundation grants 1147930 and 1321143, TEKES, Graduate School in Electronics, Telecommunications and Automation (GETA), HPY Foundation and Nokia Foundation.

M. Čierny is with Nokia Networks, 02610 Espoo, Finland (e-mail: michal.cierny@nsn.com).

Z. Ding is with Department of Electrical and Computer Engineering, University of California, Davis, California 95616 (e-mail: zding@ucdavis.edu).

R. Wichman is with Department of Signal Processing and Acoustics, Aalto University School of Electrical Engineering, 00076 Aalto, Finland (e-mail: risto.wichman@aalto.fi).

and radio link reliability. Modern cellular systems, such as 3GPP Long Term Evolution (LTE) [2], extensively rely on multiple-input and multiple-output (MIMO) techniques.

Interference is inherently a major capacity limiting factor in cellular networks and comes in quite a few shapes: intra-cell interference, inter-cell interference, interference between spatial streams for the same user, etc. In this work we focus on inter-cell interference, i.e., interference between adjacent cells, also known as other cell interference (OCI). Though it is well known in the community that spatial multiplexing is susceptible to OCI [3], the converse has not been explored well. In other words, there is little information on what effect spatially multiplexed interference may have on other types of transmissions within the system.

Our study is motived by situations when a receiver with a weak desirable signal is interfered by another transmitter that may have the option to choose the rank of its transmission for sending single-layer or multi-layer MIMO transmissions. Having such choices requires the interferer to have a strong channel to its own receiver as spatial multiplexing usually does not fare well in low signal-to-interference-plus-noise-ratio (SINR) regime. This can happen when a user equipment (UE) is near the cell edge and is being interfered by a neighbor base station (BS) serving other UEs on a strong link. In a more detailed example, a macrocell UE may be located within a coverage blind spot around a closed access femtocell [4]. In a femtocell, the short link between a transmitter and a receiver tends to be strong and chances to use spatial multiplexing can be high.

The way we approached our analysis is similar to [5] which studied the performance of beamforming. The work in [5] does not consider interferers performing spatial multiplexing or orthogonal space-time block coding (OSTBC) transmissions. We found one contribution to such mixed MIMO cases in [6] where the authors simulated a hexagonal cellular network layout and collected SINR as well as bit error rate statistics. Another related work appears in [7], which only considers signal-to-interference ratio (SIR) without channel noise and does not tackle outage probability. Performance of OSTBC under various MIMO interference has been analyzed in [8]–[10]. Similar to [7] the authors analyzed SIR distributions with neither noise nor outage probability. A simulation study that included antenna correlation is given in [11].

The difference between spatial multiplexing and beamforming transmissions is reflected in the rank of interference signal space. In this paper we analyze the impact of interference rank on the performance of a receiver whose own transmitter also applies beamforming or OSTBC. We

consider arbitrary number of interferers, each of whom with their own transmission power and multi-antenna technique. We place no limit on the number of antennas at the transmitter or the receiver. We incorporate realistic channel conditions including near-static long term component and short term Rayleigh fading. We derive a closed-form outage probability, verify its validity using Monte Carlo simulations, and use it to assess the impact of interference rank on the own transmission.

Our results suggest that higher rank transmission of a strong interferer has a lower probability of causing outage than a rank 1 interferer. When the desired user transmitter performs beamforming, this translates to more than $2\mathrm{dB}$ gain in the supported SINR threshold for high dimension MIMO receivers. With the user signal transmitter performing OSTBC, the gain is still apparent but drops below $1\mathrm{dB}$.

We specify three main contributions in our work:

- We directly show the effect of interference rank on a single layer MIMO transmission. We derive SINR and outage probability for different interference ranks. Although our analysis is built on existing results [5], this is the first known comprehensive study on interference rank.
- We extend the known results on how interferers with arbitrary multi-antenna transmission techniques affect beamforming and OSTBC transmission [10] by including noise power, as well as by deriving the probability of outage as in [5]. Hence, our analysis is not limited to interference limited scenarios and, for given outage threshold, provides a clearer performance metric.
- We offer a better insight into how precoded interference affects OSTBC own transmission than previously known [8]–[10] by deriving the mean value of the random interference, thereby justifying existing approximation.

Our paper is organized as follows. Following this introduction, Section II summarizes the system model with major assumptions. Then, in Section III we derive the SINR distribution and probability of outage of beamforming and OSTBC under arbitrary number of interferers that perform OSTBC or precoding. In Section IV we validate our SINR and outage probability to present our main results and discuss their impact. Finally Section V concludes our manuscript.

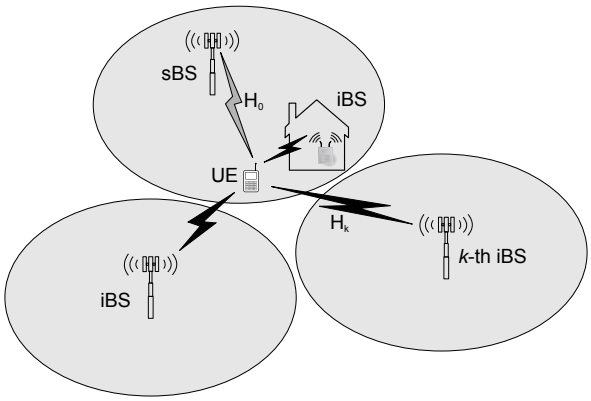

Fig. 1. An example scenario with an UE receiving its own signal from a macro sBS and interference signals from a femto iBS and two macro iBSs.

II. System Model

Consider a general cellular downlink scenario with a UE that receives its own signal from a single serving base station (sBS) and interfering signals from arbitrary number K of interfering base stations (iBSs). An illustrative scenario with a femto iBS and several macro iBSs is shown in Fig. 1. The radio channel between any link from a BS to an UE consists of a long term component, typically depending on large-scale channel models on pathloss and shadowing effect, and a small-scale Rayleigh fading component. We analyze quasi-static situations where the large scale channel parameters are constant across time and spatial subchannels, where considering the average effect of fast fading components that are flat in frequency but vary for each time instant and spatial subchannel. The spatial components of fast fading are assumed to be i.i.d.

Consider that the UE has N_{R} receive antennas and each of the BSs has N_{T} transmit antennas. We denote the long term received power of the user signal as R_0 and the long term received power of i-th iBS as R_i. Values R_0 and R_i contain all coupling gain components (transmission power, long term channel effect, noise figure, etc.) except the fast fading channel effect. The fast fading component between the UE and sBS is a $N_{\mathrm{R}} \times N_{\mathrm{T}}$ matrix $\mathbf{H}_0$ with complex Gaussian elements with zero mean and unit variance. The fast fading component between the UE and i-th iBS is a same type $N_{\mathrm{R}} \times N_{\mathrm{T}}$ matrix and is denoted by $\mathbf{H}_i$. Received signal at the UE is further corrupted by additive white Gaussian noise with power σ_{n}^2. For simplicity, we normalize the data symbols to be of unit energy.

We consider two transmission schemes in this work. In situations when a BS has reliable channel state information (CSI), it shall apply precoding, i.e., a closed-loop MIMO transmission. As focus is to assist a UEs with weak user signals (lower SINR regime), the sBS will be restricted to single-layer transmission, i.e., beamforming. The iBSs are not restricted in this way. The number of transmission layers of i-th iBS, denoted as ${N_{\mathrm{L}}}^{(i)}$, can be $1 \leq {N_{\mathrm{L}}}^{(i)} \leq \min\{N_{\mathrm{R}}, N_{\mathrm{T}}\}$. For tractability purposes we assume that sBS performs optimal beamforming based on eigen-decomposition of $\mathbf{H}_0^{\dagger}\mathbf{H}_0$. This is an ideal version of the codebook approach present in LTE. The receiver shall have accurate CSI from channel estimation and perform maximum ratio combining (MRC) reception.

In situations when BS does not have reliable CSI with respect to its downlink channel, it can utilize OSTBC, where N_{T} data symbols are encoded over N_{T} time instances. While it is known [12] that a full rate OSTBC exists only for $N_{\mathrm{T}} = 2$, we can extrapolate the results to higher N_{T} for illustrative purposes. If sBS performs OSTBC, UE applies coherent OSTBC receiver processing as shown in [13] and formalized in [12]. In case an iBS performs OSTBC its ${N_{\mathrm{L}}}^{(i)}$ is, naturally, equal to one.

III. Analysis

In this section we will analyze performance of beamforming and OSTBC under a finite number of interferers that perform precoding or OSBTC. Our ultimate performance measure shall be outage probability p_{out} defined as

$$p_{\text{out}} \triangleq \mathbb{P}\left\{\gamma \leq \gamma_0\right\} = \int_0^{\gamma_0} p_\gamma(x)dx, \tag{1}$$

where γ is post-processing SINR and γ_0 is the outage threshold. Throughout the paper we will refer to post-processing SINR simply as SINR.

For both sBS transmission modes the SINR is expressed as

$$\gamma = \frac{x}{y+1}, \tag{2}$$

where x represents received user signal power normalized by noise power and y represents received interference power normalized by noise power. Our main task is then to find distributions of independent random variables (RVs) x and y. Once we find them, we can calculate the probability density function (PDF) of SINR from

$$p_\gamma(\gamma) = \int_0^{\infty} (y+1)p_x((y+1)\gamma)p_y(y)dy \tag{3}$$

and outage probability from

$$p_{\text{out}} = \int_0^{\gamma_0} \int_0^{\infty} (y+1) p_x((y+1)\gamma) p_y(y) dy d\gamma. \tag{4}$$

Because our analysis is built in the same way as in [5] and the references within, one can also use distributions of x and y to approximate symbol error rate of some specific modulation formats. However, as this step could not be considered novel, we will leave it out of this work.

A. Outage Probability of Beamforming

A received sample vector $\mathbf{r}$ at the UE antenna ports can be expressed as

$$\mathbf{r} = \sqrt{R_0}\mathbf{H}_0\mathbf{w}_0 d_0 + \sum_{i=1}^{K} \sqrt{R_i}\mathbf{h}_{\text{eq}}^{(i)} + \mathbf{n}, \tag{5}$$

where $\mathbf{w}_0$ is a $N_{\text{T}}\times 1$ sBS precoding vector with unit Frobenius norm, d_0 is sBS data symbol, $\mathbf{h}_{\text{eq}}^{(i)}$ is $N_{\text{R}}\times 1$ equivalent channel vector of the i-th interferer and $\mathbf{n}$ is $N_{\text{R}}\times 1$ noise sample vector. The insides of $\mathbf{h}_{\text{eq}}^{(i)}$ depend on transmission technique of the i-th iBS. Assuming j-th iBS performing beamforming and k-th iBS performing spatial multiplexing, we have

$$\mathbf{h}_{\text{eq}}^{(j)} = \mathbf{H}_j\mathbf{w}_j d_j, \tag{6}$$

$$\mathbf{h}_{\text{eq}}^{(k)} = \mathbf{H}_k\mathbf{W}_k\mathbf{d}_k = \sum_{m=1}^{{N_{\text{L}}}^{(k)}} \mathbf{H}_k\mathbf{w}_{km}d_{km} = \sum_{m=1}^{{N_{\text{L}}}^{(k)}} \mathbf{h}_{\text{eq}}^{(km)}, \tag{7}$$

where $\mathbf{W}_k$ is a $N_{\text{T}}\times {N_{\text{L}}}^{(k)}$ precoding matrix with unit Frobenius norm and $\mathbf{d}_k$ is ${N_{\text{L}}}^{(k)}\times 1$ symbol vector. With k-th iBS performing spatial multiplexing we further divide the equivalent channel $\mathbf{h}_{\text{eq}}^{(k)}$ into contributions from separate transmission layers $\mathbf{h}_{\text{eq}}^{(km)}$, $m \in [1, {N_{\text{L}}}^{(k)}]$. In a case when l-th iBS performs OSTBC the equivalent channel vector could be for example

$$\mathbf{h}_{\text{eq}}^{(l)} = \frac{1}{\sqrt{N_{\text{T}}}}\mathbf{H}_l\mathbf{d}_l, \tag{8}$$

where $\mathbf{d}_l$ is $N_{\text{T}}\times 1$ symbol vector. Depending on the time instance, the insides of $\mathbf{h}_{\text{eq}}^{(l)}$ could also be a little different. However, that does not alter the derivations that will follow. We also note here that the presented options may cover other iBS transmission techniques, for example open loop spatial multiplexing [10].

Using MRC filter $\mathbf{w}_0^{\dagger}\mathbf{H}_0^{\dagger}$ we define the SINR as

$$\gamma \triangleq \frac{R_0\left\|\mathbf{w}_0^{\dagger}\mathbf{H}_0^{\dagger}\mathbf{H}_0\mathbf{w}_0\right\|^2}{\sum_{i=1}^{K}\sum_{j=1}^{{N_{\text{L}}}^{(i)}} R_i\left\|\mathbf{w}_0^{\dagger}\mathbf{H}_0^{\dagger}\mathbf{h}_{\text{eq}}^{(ij)}\right\|^2 + \left\|\mathbf{w}_0^{\dagger}\mathbf{H}_0^{\dagger}\right\|^2\sigma_{\text{n}}^2}. \tag{9}$$

$$f_\gamma(\gamma) = \sum_{i=1}^{p'} \sum_{j=1}^{t'_i} \sum_{k=1}^{M} \sum_{l=N-M}^{(N+M-2k)k} b_{ij}\varphi_{kl}\gamma^l e^{-\frac{k\gamma}{\psi_0}} \sum_{r=0}^{l+1} \binom{l+1}{r} \frac{\Gamma(r+t'_i)}{l!\Gamma(t'_i)} \left(\frac{k}{\psi_0}\right)^{l+1} \left(\frac{1}{\psi_i}\right)^{j} \left(\frac{\psi_0}{k\gamma+\Lambda_i}\right)^{r+j} \tag{19}$$

$$p_{\text{out}} = \sum_{k=1}^{M} \sum_{l=N-M}^{(N+M-2k)k} \varphi_{kl} \left(1 - e^{-\frac{k\gamma_0}{\psi_0}} \left(\frac{1}{\psi_1}\right)^{t'_1} \sum_{r=0}^{l} \sum_{s=0}^{r} \binom{r}{s} \frac{\Gamma(s+t'_1)}{r!\Gamma(t'_1)} \left(\frac{k\gamma_0}{\psi_0}\right)^{r} \left(\frac{k\gamma_0}{\psi_0} + \frac{1}{\psi_1}\right)^{-(s+t'_1)}\right) \tag{20}$$

$$p_{\text{out}} = \sum_{i=1}^{p'} \sum_{j=1}^{t'_i} \sum_{k=1}^{M} \sum_{l=N-M}^{(N+M-2k)k} b_{ij}\varphi_{kl} \left(1 - e^{-\frac{k\gamma_0}{\psi_0}} \left(\frac{\Lambda_i}{k\gamma_0+\Lambda_i}\right)^{j} \sum_{r=0}^{l} \sum_{s=0}^{r} \binom{r}{s} \frac{\Gamma(s+j)}{r!\Gamma(j)} \left(\frac{k\gamma_0}{\psi_0}\right)^{r} \left(\frac{\psi_0}{k\gamma_0+\Lambda_i}\right)^{s}\right) \tag{21}$$

As sBS uses optimal beamforming we get $\left\|\mathbf{w}_0^\dagger \mathbf{H}_0^\dagger\right\|^2 = \lambda_{\max}$, where $\lambda_{\max}$ is the dominant eigenvalue of $\mathbf{H}_0^\dagger \mathbf{H}_0$. Dividing the SINR expression from (9) by $\lambda_{\max}\sigma_{\text{n}}^2$ we get the necessary shape as in (2). The numerator RV x is given by

$$x = \psi_0 \lambda_{\max}, \tag{10}$$

where ψ_0 represents the long term SNR R_0/σ_{n}^2. Distribution of x has been found in [14] and can be expressed as

$$p_x(x) = \sum_{k=1}^{M} \sum_{l=N-M}^{(N+M-2k)k} \varphi_{kl} \frac{x^l}{\Gamma(l+1)} \left(\frac{k}{\psi_0}\right)^{l+1} e^{-\frac{xk}{\psi_0}}, \tag{11}$$

where $M = \min\{N_{\text{R}}, N_{\text{T}}\}$, $N = \max\{N_{\text{R}}, N_{\text{T}}\}$ and φ_{kl} are weight coefficients defined by

$$\varphi_{kl} = \frac{l! c_{kl}}{k^{l+1} \prod_{s=1}^{M} (M-s)!(N-s)!}, \tag{12}$$

where c_{kl} ensures that $\sum_{k=1}^{M} \sum_{l=N-M}^{(N+M-2k)k} \varphi_{kl} = 1$. Values of φ_{kl} can be found by symbolic or numeric software. For the most common antenna configurations they have been tabulated in [14].

Let us now look at the structure of y. Firstly, with k-th iBS performing beamforming or spatial multiplexing, vector $\mathbf{H}_k \mathbf{w}_{km} d_{km}$ has complex Gaussian elements with zero mean and variance $1/{N_{\text{L}}}^{(k)}$. This stems from the fact that matrices $\mathbf{W}_k$ and vectors $\mathbf{w}_k$ are normalized [15]. Similarly, multiplying given term with $\mathbf{w}_0^\dagger \mathbf{H}_0^\dagger / \left\|\mathbf{w}_0^\dagger \mathbf{H}_0^\dagger\right\|^2$ does not change Gaussianity of the elements and thus the whole term $\left\|\mathbf{w}_0^\dagger \mathbf{H}_0^\dagger \mathbf{h}_{\text{eq}}^{(km)}\right\|^2 / \left\|\mathbf{w}_0^\dagger \mathbf{H}_0^\dagger\right\|^2$ is exponentially distributed with rate ${N_{\text{L}}}^{(k)}$. Secondly, with l-th iBS performing OSTBC, $\mathbf{H}_l$ in (8) is multiplied by normalized

$\mathbf{d}_l/\sqrt{N_\mathrm{T}}$ leading to the term $\left\|\mathbf{w}_0^\dagger \mathbf{H}_0^\dagger \mathbf{h}_{\mathrm{eq}}^{(l)}\right\|^2 / \left\|\mathbf{w}_0^\dagger \mathbf{H}_0^\dagger\right\|^2$ being exponentially distributed with rate N_T.

Variable y is consequently given by a sum of weighted exponential RVs. The weights ψ_k and ψ_l, corresponding to precoding and OSTBC, respectively, are given by

$$\psi_k = \frac{R_k}{{N_\mathrm{L}}^{(k)} \sigma_\mathrm{n}^2}, \tag{13}$$

$$\psi_l = \frac{R_l}{N_\mathrm{T} \sigma_\mathrm{n}^2}. \tag{14}$$

The number of summed exponential RVs is $\sum_{m=1}^{K} {N_\mathrm{L}}^{(m)}$. We can divide the contributions into p' groups with i-th group having t_i' entries such that all entries with the same weight ψ_i are in the same group. Then, if we obtain only one group, the RV y will be gamma distributed with shape t_1' and scale ψ_1

$$p_y(y) = \frac{1}{\Gamma(t_1') \psi_1^{t_1'}} y^{t_1'-1} e^{-\frac{y}{\psi_1}}. \tag{15}$$

If we get $p'>1$ then the PDF of y can be expressed according to [16] as

$$p_y(y) = \sum_{i=1}^{p'} \sum_{j=1}^{t_i'} b_{ij} \frac{1}{\Gamma(j) \psi_i^j} y^{j-1} e^{-\frac{y}{\psi_i}}, \tag{16}$$

where the coefficients b_{ij} are

$$b_{ij} = (-1)^{t_i'+j} \sum_{\theta(i,j)} \prod_{\substack{k=1 \\ k \neq i}}^{p'} \binom{t_k'+q_k-1}{q_k} \frac{\left(\frac{\psi_k}{\psi_i}\right)^{q_k}}{\left(1-\frac{\psi_k}{\psi_i}\right)^{t_k'+q_k}}, \tag{17}$$

where $\theta(i,j)$ is a set of p'-tuples with nonnegative integers according to

$$\theta(i,j) = \left\{ (q_1 \ q_2 \ \cdots \ q_{p'}) : q_i = 0, \ \sum_{k=1}^{p'} q_k = t_i' - j \right\}. \tag{18}$$

Distributions of x and y and may now be used in (3) to derive the probability of outage. With

$p'=1$, we use (11) and (15) that leads to

$$f_\gamma(\gamma) = \int_0^\infty (y+1) \sum_{k=1}^{M} \sum_{l=N-M}^{(N+M-2k)k} \varphi_{kl} \frac{(y+1)^l \gamma^l}{l!} \left(\frac{k}{\psi_0}\right)^{l+1} \times e^{-\frac{(y+1)\gamma k}{\psi_0}} \frac{y^{t_1'-1}}{\Gamma(t_1')} \left(\frac{1}{\psi_1}\right)^{t_1'} e^{-\frac{y}{\psi_1}} dy \tag{22}$$

$$= \sum_{k=1}^{M} \sum_{l=N-M}^{(N+M-2k)k} \frac{\varphi_{kl}}{l!\Gamma(t_1')} \left(\frac{k}{\psi_0}\right)^{l+1} \left(\frac{1}{\psi_1}\right)^{t_1'} \gamma^l e^{-\frac{k\gamma}{\psi_0}} \times \int_0^\infty (y+1)^{l+1} y^{t_1'-1} e^{-y\left(\frac{k\gamma}{\psi_0}+\frac{1}{\psi_1}\right)} dy. \tag{23}$$

Now, by first applying [17, (1.111)] before using [17, (3.351.3)] we can derive the PDF of SINR as

$$f_\gamma(\gamma) = \sum_{k=1}^{M} \sum_{l=N-M}^{(N+M-2k)k} \varphi_{kl} \gamma^l e^{-\frac{k\gamma}{\psi_0}} \sum_{r=0}^{l+1} \binom{l+1}{r} \frac{\Gamma(r+t_1')}{l!\Gamma(t_1')} \times \left(\frac{k}{\psi_0}\right)^{l+1} \left(\frac{1}{\psi_1}\right)^{t_1'} \left(\frac{k\gamma}{\psi_0}+\frac{1}{\psi_1}\right)^{-(r+t_1')}. \tag{24}$$

For a general case with $p' > 1$ the PDF has been derived in [5] and is given in (19), with $\Lambda_i = \psi_0/\psi_i$. In a similar way we may use (11) and (15) or (16) in (4) to calculate the outage probability. With $p'=1$ we get

$$p_{\text{out}} = \int_0^{\gamma_0} \int_0^\infty (y+1) \sum_{k=1}^{M} \sum_{l=N-M}^{(N+M-2k)k} \varphi_{kl} \frac{(y+1)^l \gamma^l}{\Gamma(l+1)} \left(\frac{k}{\psi_0}\right)^{l+1} \times e^{-\frac{(y+1)\gamma k}{\psi_0}} \frac{y^{t_1'-1}}{\Gamma(t_1')} \left(\frac{1}{\psi_1}\right)^{t_1'} e^{-\frac{y}{\psi_1}} dy d\gamma \tag{25}$$

$$= \sum_{k=1}^{M} \sum_{l=N-M}^{(N+M-2k)k} \frac{\varphi_{kl}}{\Gamma(l+1)\Gamma(t_1')} \left(\frac{k}{\psi_0}\right)^{l+1} \left(\frac{1}{\psi_1}\right)^{t_1'} \times \int_0^\infty (y+1)^{l+1} y^{t_1'-1} e^{-\frac{y}{\psi_1}} \int_0^{\gamma_0} \gamma^l e^{-\frac{(y+1)\gamma k}{\psi_0}} d\gamma dy \tag{26}$$

We now use [17, (3.351.1)] and proceed

$$p_{\text{out}} = \sum_{k=1}^{M} \sum_{l=N-M}^{(N+M-2k)k} \frac{\varphi_{kl}}{\Gamma(t_1')} \left(\frac{1}{\psi_1}\right)^{t_1'} \int_0^\infty y^{t_1'-1} e^{-\frac{y}{\psi_1}} \times \left(1 - e^{\frac{-(y+1)\gamma_0 k}{\psi_0}} \sum_{r=0}^{l} \frac{1}{r!} \left(\frac{(y+1)\gamma_0 k}{\psi_0}\right)^r\right) dy. \tag{27}$$

Applying [17, (1.111)] and [17, (3.351.3)] we get the final form (20). Outage probability of the case with $p' > 1$ has been derived in a similar way in [5], we show it in (21).

B. Outage Probability of OSTBC

We will start the analysis of OSTBC for 2×2 MIMO case and subsequently generalize it for higher dimensions. Let us denote the received signal before filtering by

$$\mathbf{r} = \overline{\mathbf{r}} + \sum_{i=1}^{K} \tilde{\mathbf{r}}_i + \mathbf{n}, \tag{28}$$

where $\overline{\mathbf{r}}$ denotes the useful signal part and $\tilde{\mathbf{r}}_i$ denotes the interference part from i-th iBS. The useful part of the received signal may be expressed as

$$\begin{bmatrix} \overline{r}_1^{(1)} \\ \overline{r}_1^{(2)\star} \\ \overline{r}_2^{(1)} \\ \overline{r}_2^{(2)\star} \end{bmatrix} = \sqrt{R_0} \begin{bmatrix} h_{11} & h_{12} \\ h_{12}^{\star} & -h_{11}^{\star} \\ h_{21} & h_{22} \\ h_{22}^{\star} & -h_{21}^{\star} \end{bmatrix} \begin{bmatrix} d_0^{(1)} \\ d_0^{(2)} \end{bmatrix}, \tag{29}$$

where m in $\overline{r}_m^{(n)}$ represents receive antenna index, n in $\overline{r}_m^{(n)}$ represents time instance/symbol index, h_{mn} is an element of $\mathbf{H}_0$, m in $d_0^{(m)}$ represents time instance index and * denotes complex conjugate. If j-th interferer also performs OSTBC, the vector $\tilde{\mathbf{r}}_j$ will have the same structure as (29) with correspondingly different channel and symbol values. For k-th interferer performing beamforming, omitting the k index where it reduces readability, the received signal will be

$$\begin{bmatrix} \tilde{r}_1^{(1)} \\ \tilde{r}_1^{(2)} \\ \tilde{r}_2^{(1)} \\ \tilde{r}_2^{(2)} \end{bmatrix}_k = \sqrt{R_k} \begin{bmatrix} d^{(1)} \left(g_{11}w_1 + g_{12}w_2\right) \\ d^{(2)} \left(g_{11}w_1 + g_{12}w_2\right) \\ d^{(1)} \left(g_{21}w_1 + g_{22}w_2\right) \\ d^{(2)} \left(g_{21}w_1 + g_{22}w_2\right) \end{bmatrix}, \tag{30}$$

where g_{mn} denotes element of $\mathbf{H}_k$ and w_m denotes element of $\mathbf{w}_k$. For l-th interferer performing spatial multiplexing, omitting the l index where it reduces readability, we get

$$\begin{bmatrix} \tilde{r}_1^{(1)} \\ \tilde{r}_1^{(2)} \\ \tilde{r}_2^{(1)} \\ \tilde{r}_2^{(2)} \end{bmatrix}_l = \sqrt{R_l} \begin{bmatrix} d_1^{(1)}(g_{11}w_{11}+g_{12}w_{21}) + d_2^{(1)}(g_{11}w_{12}+g_{12}w_{22}) \\ d_1^{(2)}(g_{11}w_{11}+g_{12}w_{21}) + d_2^{(2)}(g_{11}w_{12}+g_{12}w_{22}) \\ d_1^{(1)}(g_{21}w_{11}+g_{22}w_{21}) + d_2^{(1)}(g_{21}w_{12}+g_{22}w_{22}) \\ d_1^{(2)}(g_{21}w_{11}+g_{22}w_{21}) + d_2^{(2)}(g_{21}w_{12}+g_{22}w_{22}) \end{bmatrix},$$

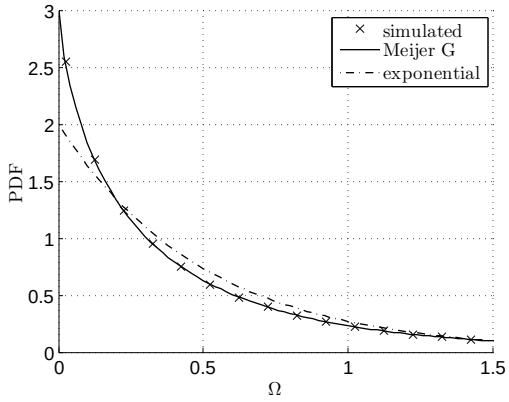

Fig. 2. Approximation of Ω_m term for outage probability of OSTBC transmission in 2×2 MIMO case with the interferer performing spatial multiplexing. Meijer G assumes Φ_m and Υ_m to be independent, exponential PDF is our final approximation.

where m in $d_m^{(n)}$ represents transmission layer index and w_{mn} is an element of $\mathbf{W}_l$. We get our symbol estimates $\hat{\mathbf{r}}$ from $\hat{\mathbf{r}}=\mathbf{Fr}$ where $\mathbf{F}$ is the receive filter

$$\mathbf{F}=\begin{bmatrix} h_{11}^{\star} & h_{12} & h_{21}^{\star} & h_{22} \\ h_{12}^{\star} & -h_{11} & h_{22}^{\star} & -h_{21} \end{bmatrix}. \tag{31}$$

The numerator RV x of (2) is known [18] to be

$$x=\frac{R_0}{4\sigma_{\mathrm{n}}^2}\left\|\mathbf{H}_0\right\|_{\mathrm{F}}^2, \tag{32}$$

where $\left\|\mathbf{H}_0\right\|_{\mathrm{F}}$ is a Frobenius norm of $\mathbf{H}_0$. Note that the quadruple noise power in the denominator of (32) comes from 1) transmission power normalization and 2) processing noise samples from two time instances at once [19]. The numerator x is hence gamma distributed with shape $N_{\mathrm{R}}N_{\mathrm{T}}$ and scale $\psi_0=R_0/{N_{\mathrm{T}}}^2\sigma_{\mathrm{n}}^2$.

$$f_\gamma(\gamma)\approx\sum_{i=1}^{p'}\sum_{j=1}^{t_i'}b_{ij}\gamma^{N_{\mathrm{R}}N_{\mathrm{T}}-1}e^{-\frac{\gamma}{\psi_0}}\left(\frac{1}{\psi_0}\right)^{N_{\mathrm{R}}N_{\mathrm{T}}}\left(\frac{1}{\psi_1}\right)^{j}\sum_{r=0}^{N_{\mathrm{R}}N_{\mathrm{T}}}\binom{N_{\mathrm{R}}N_{\mathrm{T}}}{r}\frac{\Gamma(r+j)}{\Gamma(N_{\mathrm{R}}N_{\mathrm{T}})\Gamma(j)}\left(\frac{\gamma}{\psi_0}+\frac{1}{\psi_1}\right)^{-(r+j)} \tag{42}$$

$$p_{\text{out}}\approx\sum_{i=1}^{p'}\sum_{j=1}^{t_i'}b_{ij}\left(1-e^{-\frac{\gamma_0}{\psi_0}}\left(\frac{1}{\psi_i}\right)^{j}\sum_{r=0}^{N_{\mathrm{R}}N_{\mathrm{T}}-1}\sum_{s=0}^{r}\binom{r}{s}\frac{\Gamma(j+s)}{r!\Gamma(j)}\left(\frac{\gamma_0}{\psi_0}\right)^{r}\left(\frac{\gamma_0}{\psi_0}+\frac{1}{\psi_i}\right)^{-(j+s)}\right) \tag{43}$$

The denominator RV y is a sum of RVs y_i, the shape of which is determined by the MIMO transmission technique of the interferers. If j-th interferer performs OSTBC [19], its contribution y_j is given by a sum of N_T exponentially distributed RVs with rate $1/\psi_j = {N_\mathrm{T}}^2\sigma_\mathrm{n}^2/R_j$. For k-th interferer performing beamforming we can write

$$y_k = \frac{R_k}{2\sigma_\mathrm{n}^2}\left(\Omega_1 + \Omega_2\right), \tag{33}$$

where Ω_m represent independent power contribution from m-th time instance/transmission symbol. These contributions, omitting the k index where it reduces readability, are

$$\Omega_1 = \frac{\left|h_{11}^\star d^{(1)}(g_{11}w_1+g_{12}w_2)+h_{21}^\star d^{(1)}(g_{21}w_1+g_{22}w_2)\right|^2}{\|\mathbf{H}_0\|_\mathrm{F}^2},$$

$$\Omega_2 = \frac{\left|h_{12} d^{(2)}(g_{11}w_1+g_{12}w_2)+h_{22} d^{(2)}(g_{21}w_1+g_{22}w_2)\right|^2}{\|\mathbf{H}_0\|_\mathrm{F}^2}.$$

As the data symbols and beamforming vectors are normalized to unity, $d^{(m)}(g_{n1}w_1+g_{n2}w_2)$ within numerator of Ω_m remain complex Gaussian distributed with zero mean and unit variance. However, because multiplication with elements of $\mathbf{H}_0$ is not properly normalized, i.e., the numerator of Ω_m does not contain all elements of $\mathbf{H}_0$ that are present in the denominator, the Gaussianity is lost and the distribution of Ω_m is not straightforward to establish.

We thus propose an approximation. Illustrating our approach on Ω_1, let us write $\Omega_1 = \Phi_1\Upsilon_1$, where

$$\Phi_1 = \frac{\left|h_{11}^\star d^{(1)}(g_{11}w_1+g_{12}w_2)+h_{21}^\star d^{(1)}(g_{21}w_1+g_{22}w_2)\right|^2}{|h_{11}|^2+|h_{21}|^2},$$

$$\Upsilon_1 = \frac{|h_{11}|^2+|h_{21}|^2}{\|\mathbf{H}_0\|_\mathrm{F}^2}. \tag{34}$$

The first RV Φ_1 is now properly normalized and follows exponential distribution with rate ${N_\mathrm{L}}^{(k)}$. The second RV Υ_1 can be expressed as $X/(X+Y)$ where X is gamma distributed with rate N_R and unit scale and Y is gamma distributed with rate $N_\mathrm{R}(N_\mathrm{T}-1)$ and unit scale. Variable Υ_1 therefore follows beta distribution with shape parameters $\alpha = N_\mathrm{R}$ and $\beta = N_\mathrm{R}(N_\mathrm{T}-1)$.

Variables Φ_m and Υ_m are generally not independent. For the sake of tractability we will therefore make our first approximation step and assume them to be independent. Variable Ω_m is thus given by a product of independent exponential and beta RVs. Because exponential

distribution is a special case of gamma distribution, a PDF of such product is known [20] and in our case is

$$f_{\Omega_m}(x) \approx \frac{{N_\mathrm{L}}^{(k)}\Gamma(N_\mathrm{R}N_\mathrm{T})}{\Gamma(N_\mathrm{R})} G_{1,2}^{2,0}\left(\begin{matrix} N_\mathrm{T}N_\mathrm{R}-1 \\ N_\mathrm{R}-1, 0 \end{matrix}\middle| {N_\mathrm{L}}^{(k)}x\right), \tag{35}$$

where $G_{p,q}^{m,n}$ is the Meijer G-function. Using [17, (7.811)] that states

$$\int_0^\infty x^{\rho-1} G_{p,q}^{m,n}\left(\begin{matrix} a_1,\ldots,a_p \\ b_1,\ldots,b_q \end{matrix}\middle| \alpha x\right) dx = \frac{\prod_{j=1}^{m}\Gamma(b_j+\rho)\prod_{j=1}^{n}\Gamma(1-a_j-\rho)}{\prod_{j=m+1}^{q}\Gamma(1-b_j-\rho)\prod_{j=n+1}^{p}\Gamma(a_j+\rho)}\alpha^{-\rho} \tag{36}$$

we can derive the mean value of Ω_m to be $1/N_\mathrm{T}{N_\mathrm{L}}^{(k)}$. This approximate PDF of Ω_m is not exactly convenient to work with. However, we look at its shape, as e.g. in Fig. 2, and realize it is remarkably close to that of an exponential distribution. Hence, as the second step of our approximation we assume Ω_m to take on a shape of exponential RV with rate $N_\mathrm{T}{N_\mathrm{L}}^{(k)}$. We note here that while this final shape is the same as originally proposed in [8] and subsequently used in [9], [10], our intermediate approximation (35) is novel and more precise. It also illustrates the way one comes up with the final approximation using exponential distribution in a more insightful manner.

Hence, k-th iBS, whether it performs precoding or OSTBC, contributes to y by a sum of $N_\mathrm{T}{N_\mathrm{L}}^{(k)}$ terms Ω_m. Each of the Ω_m terms is exponentially distributed with rate $1/\psi_k = {N_\mathrm{T}}^2{N_\mathrm{L}}^{(k)}\sigma_\mathrm{n}^2/R_k$, in case of OSTBC exactly and in case of precoding approximately. Now, as y is again given by a sum of weighted exponentially distributed RVs, we can divide them in p' groups such that i-th group collects all t_i' contributions that have the same weight ψ_i. Because this is the same case is in Subsection III-A, the formulas for PDF of y in (15) and (16) are valid also when UE receives OSTBC transmission.

Having PDFs of x and y ready we can use them along [17, (1.111)] and [17, (3.351.3)] in (3) to derive the PDF of SINR. With $p' = 1$, which is the case with equi-power interference

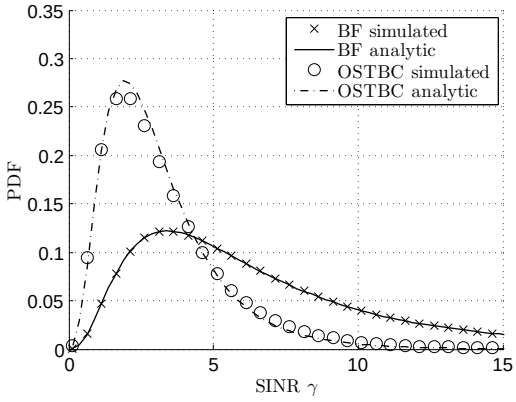

Fig. 3. SINR distribution of beamforming and OSTBC under interference from unequi-power iBSs performing different multi-antenna transmission techniques.

contributions, we get

$$f_\gamma(\gamma) \approx \gamma^{N_\mathrm{R}N_\mathrm{T}-1} e^{-\frac{\gamma}{\psi_0}} \sum_{r=0}^{N_\mathrm{R}N_\mathrm{T}} \binom{N_\mathrm{R}N_\mathrm{T}}{r} \left(\frac{1}{\psi_0}\right)^{N_\mathrm{R}N_\mathrm{T}} \times \left(\frac{1}{\psi_1}\right)^{t_1'} \frac{\Gamma(r+t_1')}{\Gamma(N_\mathrm{R}N_\mathrm{T})\Gamma(t_1')} \left(\frac{\gamma}{\psi_0}+\frac{1}{\psi_1}\right)^{-(r+t_1')}. \quad (37)$$

For a general case with $p' > 1$ the formula is given in (42). Using x and y along with [17, (3.351.1)], [17, (1.111)] and [17, (3.351.3)] we can also derive the outage probability. With $p'=1$ we get

$$p_\text{out} \approx 1 - e^{-\frac{\gamma_0}{\psi_0}} \left(\frac{1}{\psi_1}\right)^{t_1'} \sum_{r=0}^{N_\mathrm{R}N_\mathrm{T}-1} \sum_{s=0}^{r} \binom{r}{s} \frac{\Gamma(t_1'+s)}{r!\Gamma(t_1')} \times \left(\frac{\gamma_0}{\psi_0}\right)^{r} \left(\frac{\gamma_0}{\psi_0}+\frac{1}{\psi_1}\right)^{-(t_1'+s)} \quad (38)$$

and for the general case with $p'>1$ the result is given in (43).

IV. Results and Discussion

In this section we will verify the precision of our analysis from Section III by means of Monte Carlo simulations, present the main results on the effect of interference rank on beamforming and OSTBC transmission and discuss their significance and possible future work.

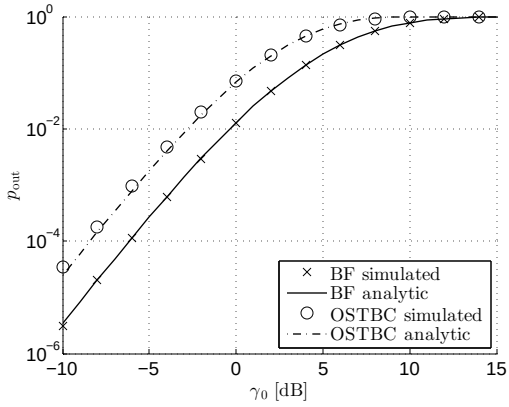

Fig. 4. Outage probability of beamforming and OSTBC under interference from unequi-power iBSs performing different multi-antenna transmission techniques, as a function of outage threshold γ_0.

A. Precision of the Analysis

In order to demonstrate that our formulas of SINR distribution and probability of outage are useful we perform Monte Carlo simulations and plot the collected statistics side by side with outputs from the formulas. The statistics are collected from 10^7 independent channel realizations. Our reference input parameters are:

- Number of receive antennas $N_{\text{R}} = 2$.
- Number of transmit antennas $N_{\text{T}} = 2$.
- Noise power $\sigma_{\text{n}}^2 = 1$.
- $\text{SNR} = 15\text{dB}$. This corresponds to long term receive user signal power of $R_0 = 31.62$.
- Interference-to-noise-ratios $\text{INR}_i = \{6\text{dB}, 8\text{dB}, 10\text{dB}\}$, corresponding to long term received interference powers of $R_i = \{3.98, 6.31, 10\}$, respectively. The first iBS performs OSTBC, the second iBS performs beamforming, and the third iBS performs spatial multiplexing, respectively.

Firstly, we consider in Fig. 3 the PDF of SINR. A mismatch between the analytical results and collected statistics may be seen at two parts of the curve that corresponds to OSTBC own transmission: the peak and the place where the right tail begins. This is due to exponential distribution used to approximate (35) as shown in Fig. 2. Overall, the formulas for PDF of SINR show a good match to the statistics collected from Monte Carlo simulations.

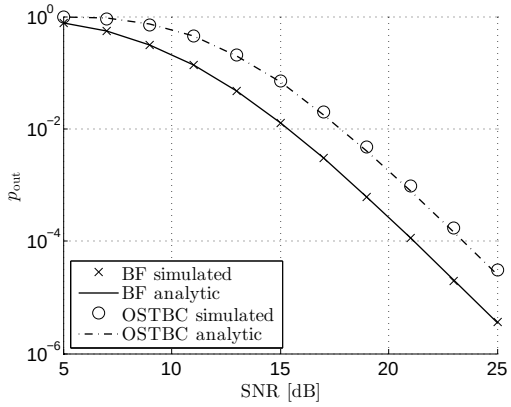

Fig. 5. Outage probability of beamforming and OSTBC under interference from unequi-power iBSs performing different multi-antenna transmission techniques, as a function of signal-to-noise-ratio.

Secondly we use Monte Carlo simulations to corroborate the analytical results on outage probability derived in Section III. In Fig. 4 we plot probability of outage as a function of γ_0 threshold whereas in Fig. 5 we provide the probability of outage as a function of SNR with $\gamma_0 = 0\mathrm{dB}$. Other parameters remain the same values as previously described. Hence, the results in Fig. 4 and Fig. 5 directly correspond to SINR distributions in Fig. 3. Our results illustrate good match between the analytical results and the simulation results. We also notice the expected performance difference between beamforming and OSTBC resulting from the presence/absence of CSI at the sBS transmitter.

B. Impact of Interference Rank

As one of our main contributions, we use the results on probability of outage in Section III to study the effect of interference rank on beamforming and OSTBC.

A typical cellular user may be interfered from many iBSs that use various multi-antenna techniques. However, only limited number of iBSs, called dominant interferers, typically have a significant impact. These are most likely iBSs that are co-located with our UE of interest, or have a strong line-of-sight spatial relation with it. Furthermore, because limiting a transmission rank of an iBS may have adverse effect on its own transmission, a single UE with weak link should not limit performance of too many neighbors. For these reasons we will draw our main insights from scenario with single iBS. We shall identify impact of multiple iBSs separately.

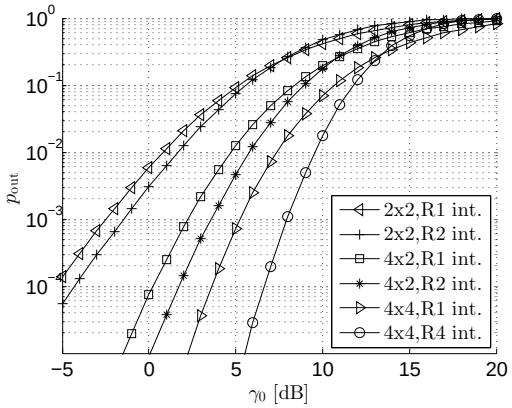

Fig. 6. Outage probability of beamforming for different antenna configurations with a single iBS performing beamforming or spatial multiplexing. In the legend, R stands for rank, specifying interference rank.

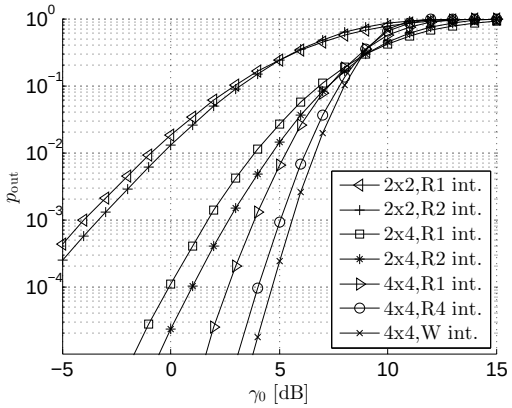

Fig. 7. Outage probability of OSTBC for different antenna configurations with a single iBS performing beamforming or spatial multiplexing. In the legend, R stands for rank of the interferer and W int. denotes white interference.

In Fig. 6 we show outage probability of beamforming with a single iBS and $\mathrm{SNR} = 15\mathrm{dB}$ and $\mathrm{INR} = 10\mathrm{dB}$. The outage probability is plotted against the γ_0 threshold, with different antenna configurations and different interference rank. For every antenna configuration the two curves (rank 1 interference vs. higher rank interference) cross each other. Hence for γ_0 above the crossing point, rank 1 interference causes lower probability of outage while with γ_0 below the crossing point, rank 1 interference leads to higher probability of outage. However, because such crossing points correspond to probability of outage well above 0.1, we can make a general

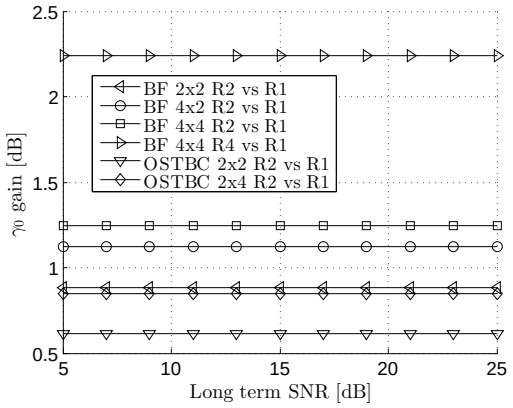

Fig. 8. Gain in the supported outage threshold under single iBS with varying long term SNR and different antenna configurations. In the legend, R stands for rank of the interferer.

observation that in the useful range of outage probability higher rank of the interference leads to lower probability of outage. This is the most interesting result of our study. The reason for this behavior stems from the fact that when an interferer transmits with higher rank, it divides available power into weaker spatial streams and lowers the possibility that much interference power may be directed towards the UE of interest. In other words, spreading the interference into multiple spatial streams leads to higher degrees of freedom in interference statistics, thereby decreasing the probability of reducing the instantaneous SINR at the UE of interest.

For the own transmission using OSTBC we show results with the same parameter settings in Fig. 7. Instead of 4×2 we consider 2×4 MIMO configuration, 4×4 is included for illustration purposes. Compared to sBS performing beamforming our observation remains the same: more degrees of freedom in higher rank interference statistics cause decrease in the probability of outage. However, the performance improvement, i.e., the increase in supported γ_0 for a given p_{out} requirement, is not as large with OSTBC as with beamforming. The reason may be found when comparing the performance with the case when interference is white. In Fig. 7 we plot one such curve, outage probability of 4×4 OSTBC transmission with white interference and the same value of $\mathrm{INR} = 10\mathrm{dB}$. The highest possible interference rank brings the performance so close to the case with white interference that there is only little space for further improvement.

Next, we studied the effect of SNR and INR on the results with single iBS. As a performance metric we used a γ_0 gain which we define as the increase in supported outage threshold γ_0

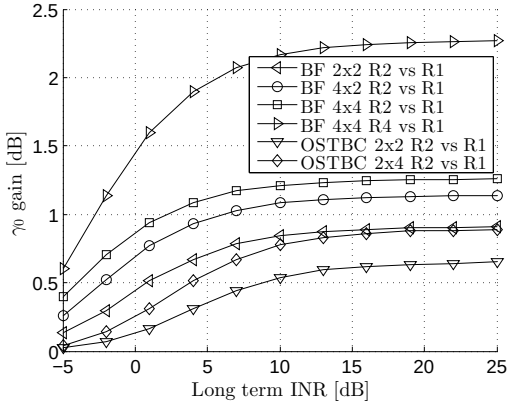

Fig. 9. Gain in the supported outage threshold under single iBS with varying long term INR and different antenna configurations. In the legend, R stands for rank of the interferer.

at given outage requirement $p_{\text{out}} = 0.01$. Visually this represents a horizontal distance between curves corresponding to rank 1 interference and higher rank interference in Fig. 6 and Fig. 7.

In Fig. 8 we show the γ_0 gain as a function of long term SNR at $\mathrm{INR} = 15\mathrm{dB}$ for different antenna configurations. The near constant SINR means that γ_0 gain is indifferent to SNR. This is because when SNR changes, SINR changes by the same amount, i.e., the curves of outage probability versus γ_0 (Fig. 6 and 7) are only shifted along the horizontal axis.

In Fig. 9 we show the γ_0 gain as a function of long term INR at $\mathrm{SNR} = 15\mathrm{dB}$ for different antenna configurations. Here the γ_0 gain is an increasing function of INR. In lower INR range, γ_0 increases faster, while in high INR range, the changes are less significant. This is because when interference is much higher than noise, changing interference power influences SINR almost as directly as changing the received user signal power (or SNR), which shifts the outage probability curve horizontally versus γ_0. The γ_0 gain also noticeably grows with higher number of transmit or receive antennas and with larger rank of the iBS transmission. When sBS performs beamforming, the γ_0 gain ranges from about $0.4\mathrm{dB}$ with 2×2 MIMO at $\mathrm{INR} = 0\mathrm{dB}$ to more than $2\mathrm{dB}$ with 4×4 MIMO at $\mathrm{INR} = 6\mathrm{dB}$ or higher. We consider the obtained gains in case of beamforming worthwhile. On the other hand, with sBS performing OSTBC the gains are relatively small, starting at around $0.25\mathrm{dB}$ at $\mathrm{INR} = 0\mathrm{dB}$ but never exceeding $1\mathrm{dB}$.

Finally, Fig. 10 shows the γ_0 gain as a function of number of iBSs at $\mathrm{SNR} = 15\mathrm{dB}$. For specific number of iBSs the interferers have equal transmission power, while across the number

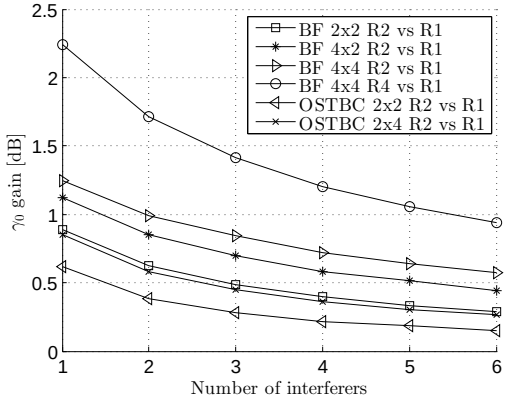

Fig. 10. Gain in the supported outage threshold versus number of iBSs with constant sum interference power and different antenna configurations. In the legend, R stands for rank of the interferers.

of iBSs we keep the total power of interference at a constant value corresponding to $\mathrm{INR}=15\mathrm{dB}$. The results show us that with more iBSs, the performance improvement from interference rank increase is smaller. This is because multiple iBSs spread the interference in space themselves. Hence, further spreading interference into spatial subchannels does not derive as much benefit as in case of single dominant interferer that uses single-layer transmission.

C. Discussion

We have shown that higher rank transmission at an iBS may serve the UE of interest better than a single rank transmission. Will it always lead to a better performance? An answer to that remains to be seen. We have provided one half of the story, that is how the interference rank affects the UE of interest. We have shown that there is potential to decrease outage of a weak link under strong interference, especially if the weak link uses beamforming as its multi-antenna technique. The other part of the story should consider the effect of the rank choice on the own transmissions of the iBSs and evaluate the issue from a system level perspective. We leave these thoughts for future consideration.

Another important issue here is how should our UE or sBS convey the request to use higher transmission to one or more iBSs. Majority of LTE BSs are equipped with the X2 interface to exchange control messages with other BSs and thus could take advantage of it. However, not all BSs have this option. For example, femto BSs are connected to the network via ADSL or

similar last mile connection that is not compatible with X2. In that case, a dedicated over-the-air interface may be needed. In our opinion, trends in cellular communications seem to be generally moving towards cooperative transmissions, therefore considering an effect of transmission rank on a neighboring reception should not be a major issue in the near future.

V. Conclusions

We have derived SINR distribution and probability of outage of beamforming and OSTBC under arbitrary number of interferers with arbitrary transmission power and several options of multi-antenna techniques. We have subsequently used these to analyze impact of interference rank on a weak link that uses beamforming or OSTBC as its transmission technique. Our results suggest that the interference statistics of higher rank transmissions positively impact performance by decreasing the probability of outage, leading to gain in the supported SINR threshold.

References

[1] E. Biglieri, R. Calderbank, A Constantinides, A. Goldsmith, A. Paulraj, H.V. Poor, "MIMO Wireless Communications," *Cambridge University Press*, 2010

[2] E. Dahlman, S. Parkvall, J. Skold, P. Beming, "3G evolution: HSPA and LTE for mobile broadband," *Academic Press*, 2010

[3] J.G. Andrews, Wan Choi, R.W. Heath, "Overcoming Interference in Spatial Multiplexing MIMO Cellular Networks," *IEEE Wireless Commun.*, vol. 14, no. 6, pp. 95-104, December 2007

[4] V. Chandrasekhar, J.G. Andrews, A. Gatherer, "Femtocell Networks: A Survey," *IEEE Commun. Mag.*, vol. 46, no. 9, pp. 59-67, September 2008

[5] K.S. Ahn, "Performance Analysis of MIMO-MRC System in the Presence of Multiple Interferers and Noise over Rayleigh Fading Channels," *IEEE Trans. Wireless Commun.*, vol. 8, no. 7, pp. 3727-3735, July 2009

[6] M.I. Rahman, E. De Carvalho, R. Prasad, "Impact of MIMO Co-Channel Interference," *IEEE 18th Int. Symp. on Personal, Indoor and Mobile Radio Commun., 2007. PIMRC 2007*, 3-7 Sept. 2007

[7] Y. Li, L. Zhang, L.J. Cimini, H. Zhang, "Statistical Analysis of MIMO Beamforming With Co-Channel Unequal-Power MIMO Interferers Under Path-Loss and Rayleigh Fading," *IEEE Trans. Signal Processing*, vol. 59, no. 8, pp. 3738-3748, August 2011

[8] Y. Li, L.J. Cimini, N. Himayat, "Performance Analysis of Space-Time Block Coding with Co-Channel MIMO Interferers," *IEEE Global Telecommun. Conf., 2008. IEEE GLOBECOM 2008*, Nov. 30 2008-Dec. 4 2008

[9] Y. Li, L. Zhang, L.J. Cimini, H. Zhang, "Impact of Arbitrary Co-Channel MIMO Modes on Alamouti Coding under Path-Loss and Rayleigh Fading," *2011 IEEE Int. Conf. on Commun. (ICC)*, 5-9 June 2011

[10] L. Zhang, Y. Li, L.J. Cimini, "Statistical Performance Analysis for MIMO Beamforming and STBC when Co-Channel Interferers Use Arbitrary MIMO Modes," *IEEE Trans. Commun.*, vol. 60, no. 10, pp. 2926-2937, October 2012

[11] D.-L. Jia, G. Wu, S.-Q. Li, "The Interference of MIMO Transmission Modes in Downlink LTE Systems," *2012 Int. Conf. on Wireless Commun. & Signal Processing (WCSP)*, 25-27 Oct. 2012

[12] V. Tarokh, H. Jafarkhani, A.R. Calderbank, "Space-Time Block Codes from Orthogonal Designs," *IEEE Trans. Inf. Theory*, vol. 45, no. 5, pp. 1456-1467, July 1999.

[13] S. M. Alamouti, "A Simple Transmitter Diversity Scheme for Wireless Communications," *IEEE J. Select. Areas Commun.*, vol. 16, pp. 1451-1458, October 1998.

[14] P.A. Dighe, R.K. Mallik, S.S. Jamuar, "Analysis of Transmit-Receive Diversity in Rayleigh Fading," *IEEE Trans. Commun.*, vol. 51, no. 4, pp. 694-703, April 2003

[15] A. Shah, A.M. Haimovich, "Performance Analysis of Maximal Ratio Combining and Comparison with Optimum Combining for Mobile Radio Communications with Cochannel Interference," *IEEE Trans. Veh. Technol.*, vol. 49, no. 4, pp. 1454-1463, July 2000

[16] X.W. Cui, Q.T. Zhang, Z.M. Feng, "Outage Performance for Maximal Ratio Combiner in the Presence of Unequal-Power Co-Channel Interferers," *IEEE Commun. Lett.*, vol. 8, no. 5, pp. 289-291, May 2004

[17] I.S. Gradshteyn and I.M. Ryzhik, "Table of Integrals, Series, and Products, 7th ed.," *Academic Press*, 2007

[18] R.U. Nabar, H. Bolcskei, A.J. Paulraj, "Diversity and Outage Performance in Space-Time Block Coded Ricean MIMO Channels," *IEEE Trans. Wireless Commun.*, vol. 4, no. 5, pp. 2519-2532, September 2005

[19] W. Choi, N. Himayat, S. Talwar, M. Ho, "The Effects of Co-channel Interference on Spatial Diversity Techniques," *IEEE Wireless Commun. and Networking Conf., 2007. WCNC 2007.*, pp. 1936-1941, 11-15 March 2007

[20] M.D. Springer, W.E. Thompson, "The Distribution of Products of Beta, Gamma and Gaussian Random Variables," *SIAM Journal on Applied Mathematics*, vol. 18, no. 4, pp. 721-737, June 1970